Biophysical Reviews (2023) 15:601–609
https://doi.org/10.1007/s12551-023-01076-3

REVIEW

Biophysical tools to study the oligomerization dynamics of Prx1-class peroxiredoxins

Sebastián F. Villar[1] · **Matías N. Möller**[1] · **Ana Denicola**[1]

Received: 14 April 2023 / Accepted: 4 June 2023 / Published online: 15 June 2023

Abstract

Peroxiredoxins (Prx) are ubiquitous, highly conserved peroxidases whose activity depends on catalytic cysteine residues. The Prx1-class of the peroxiredoxin family, also called typical 2-Cys Prx, organize as head-to-tail homodimers containing two active sites. The peroxidatic cysteine C_P of one monomer reacts with the peroxide substrate to form sulfenic acid that reacts with the resolving cysteine (C_R) of the adjacent subunit to form an intermolecular disulfide, that is reduced back by the thioredoxin/thioredoxin reductase/NADPH system. Although the minimal catalytic unit is the dimer, these Prx oligomerize into (do)decamers. In addition, these ring-shaped decamers can pile-up into high molecular weight structures. Prx not only display peroxidase activity reducing H_2O_2, peroxynitrous acid and lipid hydroperoxides (antioxidant enzymes), but also exhibit holdase activity protecting other proteins from unfolding (molecular chaperones). Highly relevant is their participation in redox cellular signaling that is currently under active investigation. The different activities attributed to Prx are strongly ligated to their quaternary structure. In this review, we will describe different biophysical approaches used to characterize the oligomerization dynamics of Prx that include the classical size-exclusion chromatography, analytical ultracentrifugation, calorimetry, and also fluorescence anisotropy and lifetime measurements, as well as mass photometry.

Keywords Peroxiredoxins · Quaternary structure · Oligomerization · SEC · Anisotropy · AUC · Lifetime fluorescence · Phasors

Introduction

Peroxiredoxins (Prx, EC 1.11.1.15) are ubiquitous, highly conserved thiol-dependent peroxidases (Wood et al. 2003a, b). A specialized Cys residue, called peroxidatic cysteine (C_P), is responsible for the reduction of the peroxide substrate (H_2O_2, peroxynitrous acid, organic hydroperoxides). The reaction of C_P with peroxides is 100 to a million times faster than the reaction of the thiol of cysteine amino acid. The topology of the active site of the Prx is essential to achieve such an increase in rate constant (Ferrer-Sueta et al. 2011). Prx are not only relevant as detoxifiers of hydroperoxides (antioxidant enzymes), but also as key players in redox signaling and modulation of cellular function, and they have been associated with several pathologies (Randall et al. 2013; Park et al. 2016; Sies 2017). For instance, Prx2 has been identified as the main antioxidant in red blood cells, keeping the concentration of H_2O_2 at subnanomolar levels (Low et al. 2007; Orrico et al. 2018). The deletion of Prx2 in model mice leads to anemia, indicating an important role in erythropoiesis (Johnson et al. 2010).

Based on the number of Cys residues participating in catalysis, Prx were classified as 2-Cys Prx (typical and atypical, forming an inter or intramolecular disulfide, respectively), and 1-Cys Prx. Based on sequence and structure around the active site, Prx are classified in six subfamilies (AhpC/Prx1, BCP/PrxQ, Tpx, Prx5, Prx6, AhpE) with different substrate and ligand specificity, sensitivity to hyperoxidation, as well as oligomeric structure (Nelson et al. 2011). There are six isoforms in humans, cytosolic Prx1, Prx2, Prx6, mitochondrial Prx3, Prx5, and Prx4 in the endoplasmic reticulum.

The catalytic cycle of Prx can be summarized in three steps: oxidation (1), resolution (2 and 3), and reduction (4) as shown in Fig. 1 for the Prx1-class. The C_P reacts with peroxide and gets oxidized to sulfenic acid (C_P-SOH) that

✉ Ana Denicola
denicola@fcien.edu.uy

[1] Laboratorio Fisicoquímica Biológica, Instituto de Química Biológica, Facultad de Ciencias, Universidad de la República, Montevideo, Uruguay

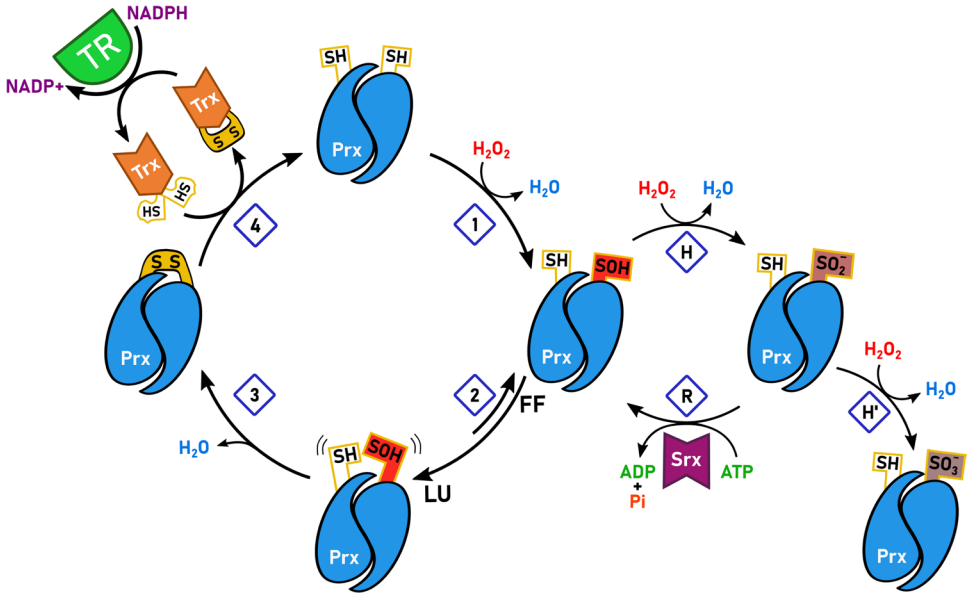

Fig. 1 Catalytic cycle of Prx1-class peroxiredoxins. Steps 1 to 4 represent the peroxidase cycle. Step 1, oxidation of C_P by the peroxide substrate. Step 2 represents the fully-folded FF to locally unfolded LU conformational transition. Step 3, intermolecular disulfide formation. Step 4, reduction by the thioredoxin Trx, thioredoxin reductase TR, NADPH system. H and H' depict the two steps of C_P hyperoxidation, while R indicates the rescue of C_P-SO_2^- by sulfiredoxin (Srx), back to the peroxidase cycle

suffers a conformational change (from a fully folded FF to a locally-unfolded LU state) to get closer to the resolving Cys (C_R) of the neighboring monomer to form an intermolecular disulfide. The disulfide is reduced by thioredoxin, that is reduced by thioredoxin reductase and NADPH (Trx/TR/NADPH system). The C_P-SOH can also react with peroxide to form sulfinic (C_P-SO_2^-) and then sulfonic acid (C_P-SO_3^-), that inactivates the peroxidase activity. Only the C_P-SO_2^- form can be rescued by sulfiredoxin (Srx) at the expense of ATP (Forshaw et al. 2021).

Quaternary structure and oligomerization dynamics of peroxiredoxins

All Prx are ~ 22 kDa globular proteins with a common Trx-fold, and display quaternary structure (Fig. 2). The minimal unit of 2-Cys Prx is a head to tail homodimer containing 2 active sites, in equilibrium with decamer (Prx1, Prx2, Prx4) or dodecamer (Prx3). Prx5 is an atypical 2-Cys Prx forming an intramolecular disulfide when oxidized, nevertheless, the reduced as well as the oxidized form arranged

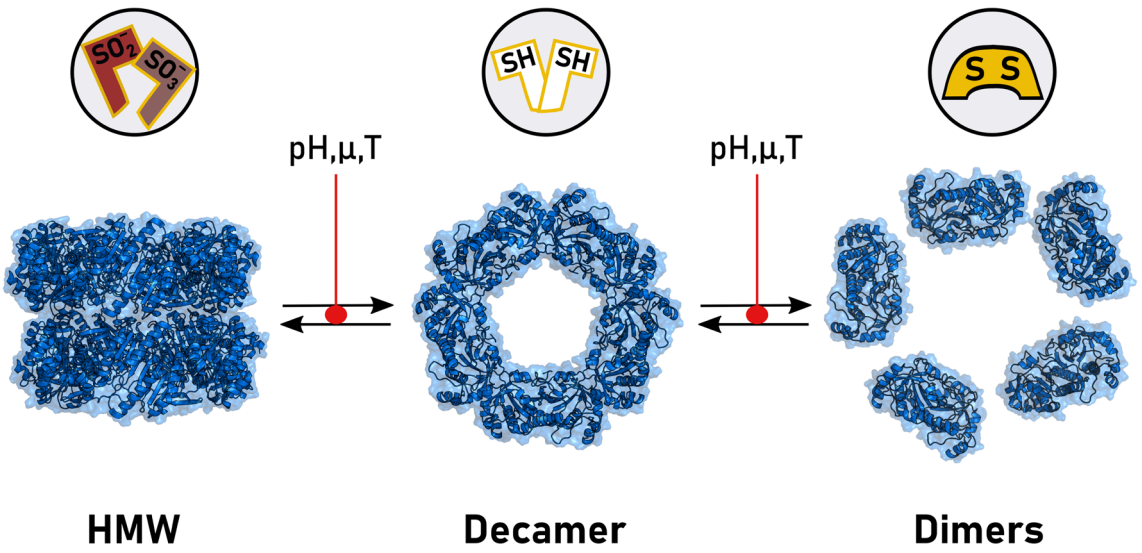

Fig. 2 Oligomerization equilibria of Prx1-class peroxiredoxins. The redox state of the active site cysteines is represented above each oligomeric form. For the hyperoxidized high-molecular-weight HMW, only the redox state of the C_P was represented. Besides the redox state of the reactive cysteines, the oligomeric state can be affected by pH, ionic strength (μ) and temperature (T), among other factors that are discussed in the text. The representations were built using PDB:7KIZ as the starting structure

as homodimers. Prx6 is a 1-Cys Prx containing only the peroxidatic Cys, but also it is present as a dimer (Table 1). Structures of related peroxiredoxins have been summarized in recent reviews (Bolduc et al. 2021; Troussicot et al. 2021).

The studies of Prx by crystallography and X-ray diffraction provided the basis for our understanding of their structure, and also information on their oligomerization states, because identifies dimers, decamers, and even dodecamers. However, it does not allow the determination of thermodynamic parameters such as the dissociation constant of those oligomers.

In the oxidized state and low protein concentration, 2-Cys Prx are mainly found as covalently disulfide-linked homodimers. At higher concentrations or when the cysteines are reduced or hyperoxidized, dimers associate into doughnut-shaped decamers (Wood et al. 2003a, b). In addition, the formation of Prx HMW aggregates has been associated with a holdase, chaperone-like activity of these enzymes that still needs deeper studies (Jang et al. 2004, Rhee et al. 2011, Veal et al. 2018, Troussicot et al. 2021).

The decamer-dimer transition is a reversible process that depends on protein concentration and other factors that has only been characterized thermodynamically (K_D determination) in a few cases. The main reason is probably that the biophysical methods used to analyze quaternary structure of proteins have different limitations that complicate the determination of the precise oligomer distribution at equilibrium (Manta et al. 2011). Different biophysical approaches used to assess Prx1-class oligomerization will be discussed below.

Size-exclusion chromatography (SEC) separates proteins according to their hydrodynamic radii. The stationary phase consists of a porous material, such that very large molecules will be sterically impeded from diffusing into the porous stationary phase and will exit the chromatography column very rapidly. Very small molecules can freely diffuse into the stationary phase and will access a larger volume and elute later. Intermediate size molecules will partially enter the stationary phase and will elute at intermediate times, according to their size. Using stationary phase with an appropriate pore size, there is an inverse linear relation between the logarithm of the molecular mass of the proteins and the retention time. This is true for globular proteins, whereas elongated proteins will appear larger because of the larger hydrodynamic radius. This confounding factor may be avoided by coupling SEC to a MALS detector, which can determine the molecular mass of the eluting compound independent of the hydrodynamic radius. One of the main advantages of SEC is that it allows rapid estimation of the molecular mass of proteins in solution, thus allowing the estimation of oligomerization state. When the oligomers are very stable, the SEC shows a single peak that allows the estimation of number of subunits in the native quaternary structure of the protein in solution. When oligomers have medium to low stability, the dissociation of the oligomer can be observed as a tailing of the main peak in the chromatogram, or by the presence of a low-molecular-weight peak, and a "bridge" connecting both peaks (Villar et al. 2022). The "bridge" indicates that the oligomer is dissociating as the chromatography is occurring, complicating the calculation of dissociation constants.

Using a small column (Superdex 200 5/150 GL column, Cytiva) at 25 °C and a fluorescence detector, it was found that reduced human Prx1 appears mostly as a decamer at total protein concentrations above 2 μM, and as dimer below 2 μM. The concentration of monomer at which subunits are equally distributed between dimers and decamers ($C_{0.5}$) was estimated as 1.3 ± 0.7 μM, with $K_D = (8.6 \pm 4.6) \times 10^{-25}$ M^4 (Villar et al. 2022). Some sequence changes were observed that modified the quaternary structure of Prx1. For instance, phosphorylation of Thr 90, or its replacement by phosphorylation mimic Asp, led to the formation of HMW aggregates (higher than 700 kDa, lower than 2000 kDa according to SEC)(Jang et al. 2006).

Using a Superdex 200 10/300 column at 25 °C, it was found that reduced human Prx2 was mostly present as a

Table 1 Crystallographic structures of human Prx

Isoform	Redox state	PDB ID	Oligomeric state	Reference
Prx1 C83S	Disulfide C_P-C_R	4XCS	dimer	(Cho et al. 2015)
Prx2	C_P-SO_2H	1QMV	decamer	(Schröder et al. 2000)
	Disulfide C_P-C_R	5IJT	decamer	(Bolduc et al. 2018)
	C_P-SH	7KIZ	decamer	(Peskin et al. 2021)
Prx3	C_P-SH	5JCG	dodecamer	(Yewdall et al. 2016)
Prx4	C_P-SH	3TKP	decamer	(Wang et al. 2012)
	Disulfide C_P-C_R	3TJB	decamer	(Cao et al. 2011)
	C_P-SO_2H	3TKQ	decamer	(Wang et al. 2012)
Prx5	C_P-SH	1H4O	dimer	(Evrard et al. 2001)
	Disulfide C_P-C_R	1OC3	dimer	(Evrard et al. 2004)
Prx6	C_P-SH	5B6M	dimer	(Kim et al. 2016)
	C_P-SOH	5B6N	dimer	(Kim et al. 2016)

decamer at concentrations above 10 µM, but dissociation to dimers appeared at lower concentrations. Because of absorbance detection limitations, the lower concentration of protein used was 5 µM monomer. The results were used to estimate $K_D = 10^{-24}$ M^4, $C_{0.5} \sim 2$ µM (Manta et al. 2009). A recent report also shows that reduced Prx2 eluted as a decamer, while oxidized Prx2 showed both decamers and dimers (Peskin et al. 2021) similar to porcine Prx2 (Schröder et al. 1998). Reduced mutants in resolving cysteine C172S, C172D, C172W resulted in higher dissociation to dimers than the wild-type (Peskin et al. 2021). Hyperoxidized human Prx2 crystallographic structure showed a similar active site to reduced Prx2 (Schröder et al. 2000), that stabilizes the dimer-dimer interface and promotes decamerization and HMW aggregate formation.

Human Prx3 forms a dodecamer in the reduced state (by X-Ray diffraction) that dissociates to dimers when oxidized (by SEC) (Cao et al. 2011). Human Prx4 was found to be a decamer, both in the reduced and the oxidized state (by SEC and X-Ray diffraction (Cao et al. 2011).

Therefore, SEC is very useful at providing information on the oligomeric state of Prx, and to study factors that affect it. However, from the model fitting, it is evident that SEC is not the most precise method to measure the K_D, because intrinsic dilution during the chromatography leads to dissociation in the column (Villar et al. 2022). This problem is further aggravated in larger columns.

Analytical ultracentrifugation (AUC) is one of the powerful techniques available for the quantitative characterization of macromolecular associations in solution. There are two approaches, sedimentation velocity (SV), and sedimentation equilibrium (SE). In SV, the transport of the macromolecule at high centrifugal force is followed and components separated on the basis of differences in mass, density, and shape. Free software is available for the analysis of the experimental time-dependent concentration gradients that allows the estimation of the molar mass and sedimentation coefficient of each sedimenting species. If the dynamics of the association/dissociation is fast and it is not possible to separate different oligomeric states on the time scale of the experiment, the SE approach could help. In SE, lower centrifugal forces are used until the equilibrium between sedimentation and diffusion is reached, thus, there is no net transport of the macromolecule. Analysis of the concentration gradient achieved at equilibrium provides information about the molar mass, stoichiometry/thermodynamics of the association. A review by P. Schuck in *Biophysical Reviews* (Schuck 2013) describes the fundamentals of SE, SV, and applications to study protein–protein interactions, not only protein self-association but also multi-protein complex formation.

AUC has been used to study structure/activity relationship and find a link between Prx oligomeric states and peroxidase activity. Early on, it was shown by AUC that *Salmonella typhimurium* AhpC was mainly in decameric form when reduced, and dissociated to dimers when oxidized (Wood et al. 2002). This was supported by dynamic light scattering, DLS, measurements. However, crystals of the oxidized protein showed decamers instead of the expected dimers, likely because the high concentration needed to crystallize the protein shifted the equilibrium to decamers. In this work, the authors were the first to suggest that Prx antioxidant and signaling activities could be regulated by the oxidation of the Prx and by the dissociation of the decamer to dimers (Wood et al. 2002).

Using AUC, reduced human Prx2 in solution was found to be mainly a decamer, although no dissociation constant could be calculated because free dimer concentration was too low to measure (Schröder et al. 2000). A 2–3 S sedimentation coefficient for the dimer, and around 8 S value for the decamer of Prx2 were reported (Randall et al. 2016; Peskin et al. 2021). Mutations on the dimer-dimer interface (C83S of hPrx1) or at the C-terminal, like the resolving C172 of Prx2, as well as post- translational modifications like glutathionylation of C83 of Prx1 or nitration of Y193 of Prx2, provoke a disruption of the decamer as evidenced by SV-AUC, with concomitant decrease on H_2O_2 reactivity (Park et al. 2011; Randall et al. 2016; Peskin et al. 2021).

Thus, AUC is very useful to study the oligomerization status of Prx. However, because these experiments have to be performed at high protein concentrations, the dissociation into dimers that occurs at very low protein concentration may not be observed and thus preclude the calculation of K_D.

Isothermal titration calorimetry (ITC) directly measures the energy associated with a biochemical reaction or a molecular interaction at constant temperature, and it has been widely used in biosciences to study thermodynamics of protein–ligand, and protein–protein interactions (Leavitt et al. 2001). A particular case is protein self-association, where the strength of the interaction can be measured in ITC dilution experiments. The stepwise addition of a concentrated solution of the protein (50–100 µM) to the calorimetric cell containing buffer, with the subsequent dilution of the macromolecule, triggers the dissociation, leading the system through a sequence of equilibrium states. The heat associated with each injection is proportional to the increment in the concentration of monomer in the calorimetric cell. As the protein concentration in the calorimetric cell progressively increases, the dissociation process is less favored, and the sequence of injections proceeds until no significant heat is detected. The total concentration of the protein needs to be precisely determined (known independent variable). Nonlinear regression analysis of the dependent variable (heat associated with each injection) allows the estimation of the thermodynamic parameters, not only the equilibrium dissociation

constant K_D, but also the enthalpic and entropic components ΔH_D, ΔS_D.

Barranco-Medina et al. (Barranco-Medina et al. 2008) studied by ITC the dimer-decamer equilibrium of 2-Cys Prx (human and plants) obtaining values of CTC (critical transition concentration) in the very low micromolar range, observing a sharp transition above this concentration that suggests a cooperative effect. Their results indicate that oligomerization of reduced 2-Cys Prx takes place at total protein concentrations lower than 2 µM. The measured positive solvation enthalpy due to the release of very ordered water molecules from dimer-decamer interface, confirmed the endothermic nature of Prx oligomerization. The oligomerization of Prx is then driven by entropy, most likely a hydrophobic effect where the release of highly ordered water in hydrophobic dimer-dimer surfaces compensates for the loss of dimer freedom and the positive enthalpy. Interestingly, no heterocomplexes with subunits from different Prx species were observed.

Mass photometry is based on interferometric scattering microscopy (Young et al. 2018), where the amount of scattered light is directly related to the mass of the molecule. It allows the determination of proteins in their native state in solution and because it is based on single molecule measurements, it can determine the mass and amounts of different molecules in a mixture, similar to DLS (dynamic light scattering), but with a higher sensitivity and resolution, thus, a much lower volume requirement. The method is limited to protein concentration below 3 µM, and to proteins larger than 40 kDa (Young et al. 2018).

Using mass photometry, it was shown that human Prx1 had a $C_{0.5} = 500$ nM at pH 8.0, whereas *A. thaliana* 2CPA had a $C_{0.5} \sim 20$ nM (Liebthal et al. 2021). In the case of *A. thaliana* 2CPA, different mutants were used to study the substitution of amino acid residues of interest in the quaternary structure. Neutral substitutions in the active site (C54S) had no effect on the quaternary structure, whereas substituting cysteine 54 for aspartate (C54D) that mimics hyperoxidation of the cysteine to sulfinic acid, led to stabilization of the decamer and the formation of HMW aggregates. Disturbing the dimer-dimer interface by replacing a phenylalanine with a charged arginine (F84R), led to stabilizing the dimers instead. Thus, mass photometry has the potential to be a powerful tool to study the factors affecting Prx oligomerization. The only concern is that the adsorption on the glass, necessary to see the scattering by this method, changes the dissociation equilibria of the species involved.

Fluorescence techniques can be extremely helpful to study the oligomerization dynamics of proteins. Förster resonance energy transfer (FRET) has been widely used to study protein–protein interactions in this context, as it is used to assess the proximity between molecules. It consists of the nonradiative transfer of the emission energy from a donor fluorophore to an acceptor, that has an excitation spectrum overlapping the donor´s emission spectrum. A two-step FRET approach was used to detect the decamer formation of plant 2-Cys Prx1 in protoplasts (Seidel et al. 2010). Herein, three GFP (green-fluorescent protein) derivatives (CFP, YFP and mCherry) where fused to the *A. thaliana* 2-Cys Prx1 and expressed at the same time to detect the two-step FRET (energy transfer from CFP to mCherry through YFP) from the different fusions localized in the same decamer. An increase in mCherry fluorescence was found, proving the formation of decamers of 2-Cys Prx1 in vivo.

Additionally, fluorescence polarization (or anisotropy) is often a helpful method since it increases as the mobility of the fluorophore decreases. Thus, oligomer formation can be assessed by following an increase in the polarization, since there is a decrease in the mobility from the free subunits to the assembled oligomer (Jameson et al. 2010). This approach has been applied to the study of the oligomerization dynamics of human Prx2 in living human cells throughout oxidation/reduction cycles (Pastor-Flores et al. 2020). Herein they transfected the cells with a fusion between Prx2 and mCerulean (hPrx2-mCer) and followed the changes in the polarization of fluorescence emission of the latter. The addition of H_2O_2 was followed by an increase in the polarization of Prx2-mCer, which later decreased to the basal state after the probe was reduced. Here, the oxidized dimers polarized the emission while the emission of the reduced decamers was depolarized. This unexpected behavior was caused by the homoFRET between neighboring mCer in the Prx2 decamer. Using this construct, a $C_{0.5} = 1$ µM can be estimated (Pastor-Flores et al. 2020).

The use of genetically encoded fluorophores is helpful to follow the oligomerization dynamics in living cells as exemplified above; however, the chemical or genetic attachment of fluorophores to a protein could potentially disturb its quaternary structure and produce oligomerization artifacts. A less intrusive approach is the study of the intrinsic fluorescence of proteins, governed by the tryptophan, Trp residue. Trp emission demonstrated to be a reliable reporter of protein structural changes since it is easily affected by physicochemical variations in its molecular environment. Figure 3A shows the change of Prx1 spectral center of mass upon a 40-fold dilution. Dilution affects the dynamics of protein oligomerization tilting the equilibrium towards dimers, noticed as a subtle red shift in the emission of Prx1. Nevertheless, the lifetime of fluorescence emission (τ) shows a larger change after dilution (Fig. 3B). The lorentzian distributions used to fit fluorescence lifetime data indicate that an important change is occurring, but it is still difficult to make use of it.

The phasor analysis of τ, is a suitable approach to study protein oligomerization, because it can be used to calculate the fraction of distinct fluorophores within a mixture. After

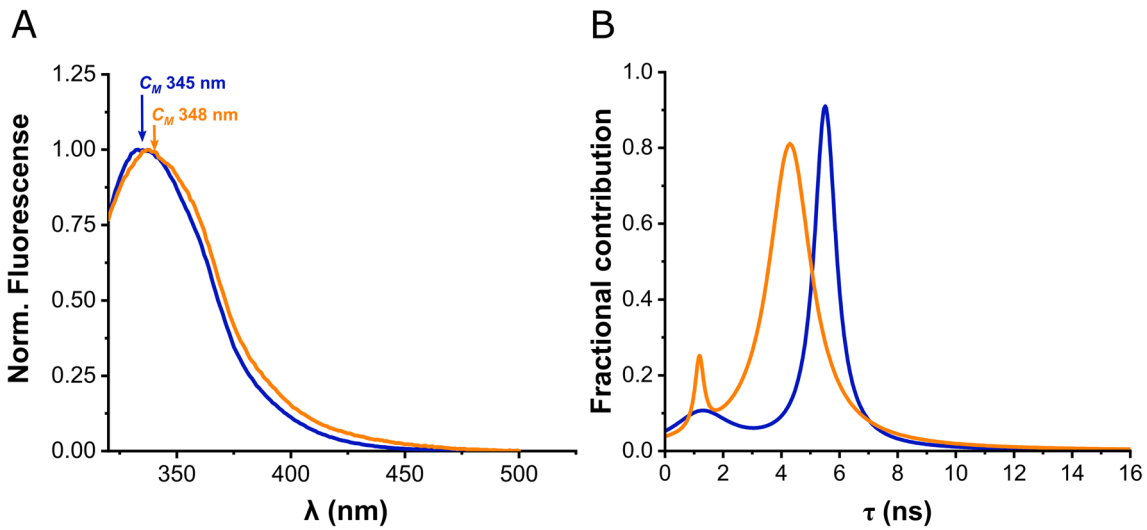

Fig. 3 Intrinsic fluorescence of hPrx1. **A** Normalized emission spectra of 20 µM (blue, mostly decamer) and 0.5 µM (orange, mostly dimer) reduced hPrx1 (λex 295 nm). The spectral center of mass (C_M) of each spectrum is indicated. **B** Lorentzian distributions obtained from the fitting of the emission lifetimes of hPrx1 20 µM (blue, decamer) and 0.5 µM (orange, dimer) obtained by frequency-domain fluorometry (LED 295 nm) (Villar et al. 2022)

the phasor transform is applied to τ data, two values named G and S are obtained. The latter are the equivalent of x and y in a Cartesian coordinate axis. The phasor plot is delimited by a semicircle (called "universal circle") that represents the position of all the fluorophores with monoexponential decays, whereas multiexponential decays will fall inside (red line in Fig. 4A). Hence, in the case of proteins, their phasors will most likely fall inside the universal circle given the complex nature of protein Trp emission. The phasor analysis allowed the calculation of the fraction of reduced Prx1 dimers and decamers at different protein concentrations (Villar et al. 2022). Prx1 dimers and decamer had distinct and spatially separated phasors that fell inside the universal circle (0.5 and 80 µM points in Fig. 4A). Mixtures of dimers and decamers had their phasors aligned on the line segment that separated dimers from decamers (1 µM point in Fig. 4A), meaning that each mixture is a linear combination of the dimer and decamer phasors. Using phasor algebra, the fraction of each oligomeric species was calculated at the assayed Prx1 concentrations, and a dissociation curve was built to obtain a K_D of 1.1×10^{-24} M^4 and a $C_{0.5}$ of 1.36 µM (Fig. 4B).

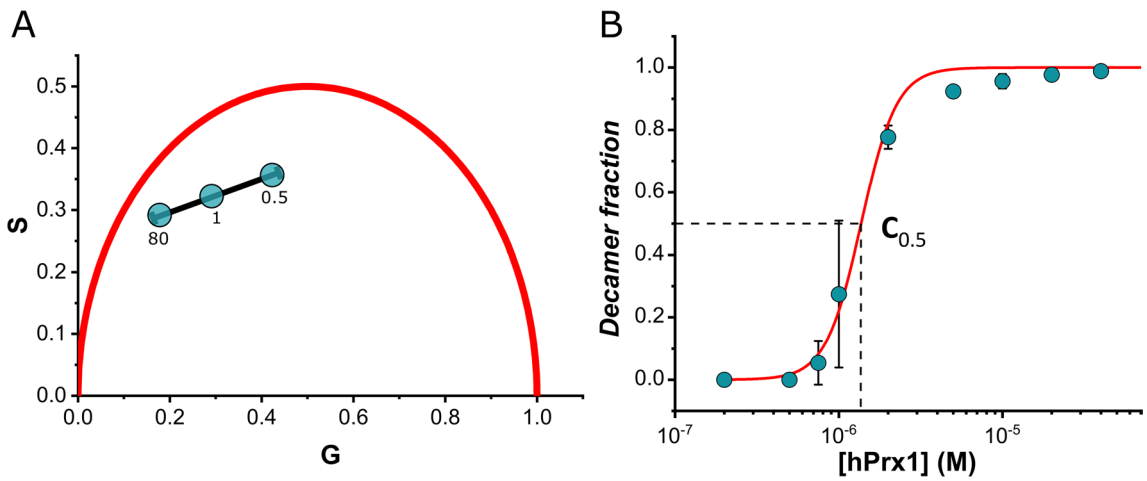

Fig. 4 Study of hPrx1 decamer-dimer equilibrium using the fluorescence lifetime phasor analysis. **A** Phasor plot for three concentration points (0.5, 1, 80 µM) of reduced hPrx1. The universal circle is delimited in red, the line segment between the dimer and decamer regions at 0.5 and 80 µM hPrx1 (confirmed by SEC) is represented in black. **B** Dissociation curve plotted as the fraction of hPrx1 decamer vs. total protein concentration. Both figures are adapted from (Villar et al. 2022)

The phasor approach is relatively simple when the system has a binary behavior, i.e., when there are only two fluorophores in the mixture (in this case, decamer and dimer). The complexity of data analysis and interpretation increases with the number of τ components.

Factors affecting oligomerization

Several factors have been reported to affect Prx oligomerization (Fig. 2), including ionic strength (Kitano et al. 1999, Chauhan et al. 2001), pH (Kristensen et al. 1999), calcium (Allen et al. 1979, Plishker et al. 1992), as well as the redox state of the active cysteines (Schröder et al. 1998, 2000; Wood et al. 2002). Reduction of the active-site disulfide is emerging as the primary factor in the stabilization of the decamer (Wood et al. 2003a, b). Total concentration of protein is a key factor that governs the oligomeric equilibria. Intracellular concentration of Prx is generally high but varies depending on the isoform present on each tissue and subcellular organelle. An extreme case is the concentration of hPrx2 in erythrocytes reported in the 250–410 µM range (Moore et al. 1991; Cho et al. 2010).

Concluding remarks

In recent years, new and exciting advances have been made regarding the role of Prx in keeping the redox status of the cell. The quaternary structure of Prx, and moreover, the transition between oligomers, is determinant on defining protein–protein interactions that are essential to achieve their biological functions. It is very likely that different proteins interact with Prx in its dimeric, decameric or HMW forms. Multiple factors can modulate the oligomeric transitions of Prx1-class Prx such as redox state, post-translational modifications, ionic strength, pH, as well as total monomer concentration. Besides the classical methods for analyzing oligomers distribution like SEC, new more precise approaches have emerged like mass photometry and fluorescence lifetime phasors that are promising to understand the dynamics of Prx oligomerization. These thermodynamic data will allow in silico simulation of the different cellular processes and contribute to understanding the biological functions of Prx.

Author contribution Conceptualization, A.D.; funding acquisition, S.F.V., M.N.M. and A.D.; visualization, S.F.V. and M.N.M.; writing – original draft, A.D.; writing – review & editing, S.F.V., M.N.M., and A.D**.** MNM and AD contributed equally to the writing and revision of this review. S.F.V. created all the figures. All authors have given approval to the final version of the manuscript.

Funding This work was supported by grants from Universidad de la República CSIC I + D Grupos 46725 to A.D., CSIC I + D to M.N.M. and CSIC iniciación to S.F.V.

Declarations

Ethical approval This article does not contain any studies with human participants or animals performed by any of the authors.

Conflict of interest The authors declare no competing interests.

References

Allen DW, Cadman S (1979) Calcium-induced erythrocyte membrane changes The role of adsorption of cytosol proteins and proteases. Biochim Biophys Acta 551(1):1–9. https://doi.org/10.1016/0005-2736(79)90348-1

Barranco-Medina S, Kakorin S, Lazaro JJ, Dietz KJ (2008) Thermodynamics of the dimer-decamer transition of reduced human and plant 2-cys peroxiredoxin. Biochemistry 47(27):7196–7204. https://doi.org/10.1021/bi8002956

Bolduc J, Koruza K, Luo T, MaloPueyo J, Vo TN, Ezeriņa D, Messens J (2021) Peroxiredoxins wear many hats: factors that fashion their peroxide sensing personalities. Redox Biol 42:101959. https://doi.org/10.1016/j.redox.2021.101959

Bolduc JA, Nelson KJ, Haynes AC, Lee J, Reisz JA, Graff AH, Clodfelter JE, Parsonage D, Poole LB, Furdui CM, Lowther WT (2018) Novel hyperoxidation resistance motifs in 2-Cys peroxiredoxins. J Biol Chem 293(30):11901–11912. https://doi.org/10.1074/jbc.RA117.001690

Cao Z, Tavender TJ, Roszak AW, Cogdell RJ, Bulleid NJ (2011) Crystal structure of reduced and of oxidized peroxiredoxin IV enzyme reveals a stable oxidized decamer and a non-disulfide-bonded intermediate in the catalytic cycle. J Biol Chem 286(49):42257–42266. https://doi.org/10.1074/jbc.M111.298810

Chauhan R, Mande SC (2001) Characterization of the Mycobacterium tuberculosis H37Rv alkyl hydroperoxidase AhpC points to the importance of ionic interactions in oligomerization and activity. Biochem J 354(Pt 1):209–215. https://doi.org/10.1042/0264-6021:3540209

Cho CS, Kato GJ, Yang SH, Bae SW, Lee JS, Gladwin MT, Rhee SG (2010) Hydroxyurea-induced expression of glutathione peroxidase 1 in red blood cells of individuals with sickle cell anemia. Antioxid Redox Signal 13(1):1–11. https://doi.org/10.1089/ars.2009.2978

Cho KJ, Park Y, Khan T, Lee J-H, Kim S, Seok JH, Chung YB, Cho AE, Choi Y, Chang T-S, Kim KH (2015) Crystal structure of dimeric human peroxiredoxin-1 C83S mutant. Bull Kor Chem Soc 36(5):1543–1545. https://doi.org/10.1002/bkcs.10284

Evrard C, Capron A, Marchand C, Clippe A, Wattiez R, Soumillion P, Knoops B, Declercq J-P (2004) Crystal structure of a dimeric oxidized form of human peroxiredoxin 5. J Mol Biol 337(5):1079–1090. https://doi.org/10.1016/j.jmb.2004.02.017

Evrard CBV, Namur SA, Clippe A, Bernard A, Knoops B (2001) Crystal structure of human peroxiredoxin 5, a novel type of mammalian peroxiredoxin at 1.5 Å resolution. J Mol Biol 311:751–759. https://doi.org/10.1006/jmbi.2001.4853

Ferrer-Sueta G, Manta B, Botti H, Radi R, Trujillo M, Denicola A (2011) Factors affecting protein thiol reactivity and specificity in peroxide reduction. Chem Res Toxicol 24(4):434–450. https://doi.org/10.1021/tx100413v

Forshaw TE, Reisz JA, Nelson KJ, Gumpena R, Lawson JR, Jonsson TJ, Wu H, Clodfelter JE, Johnson LC, Furdui CM and Lowther WT (2021). Specificity of human sulfiredoxin for reductant and peroxiredoxin oligomeric state. Antioxidants (Basel) 10(6). https://doi.org/10.3390/antiox10060946

Jameson DM, Ross JA (2010) Fluorescence polarization/anisotropy in diagnostics and imaging. Chem Rev 110(5):2685–2708. https://doi.org/10.1021/cr900267p

Jang HH, Kim SY, Park SK, Jeon HS, Lee YM, Jung JH, Lee SY, Chae HB, Jung YJ, Lee KO (2006) Phosphorylation and concomitant structural changes in human 2-Cys peroxiredoxin isotype I differentially regulate its peroxidase and molecular chaperone functions. FEBS Let 580(1):351–355. https://doi.org/10.1016/j.febslet.2005.12.030

Jang HH, Lee KO, Chi YH, Jung BG, Park SK, Park JH, Lee JR, Lee SS, Moon JC, Yun JW, Choi YO, Kim WY, Kang JS, Cheong GW, Yun DJ, Rhee SG, Cho MJ, Lee SY (2004) Two enzymes in one; two yeast peroxiredoxins display oxidative stress-dependent switching from a peroxidase to a molecular chaperone function. Cell 117(5):625–635. https://doi.org/10.1016/j.cell.2004.05.002

Johnson RM, Ho Y-S, Yu D-Y, Kuypers FA, Ravindranath Y, Goyette GW (2010) The effects of disruption of genes for peroxiredoxin-2, glutathione peroxidase-1, and catalase on erythrocyte oxidative metabolism. Free Radic Biol Med 48(4):519–525. https://doi.org/10.1016/j.freeradbiomed.2009.11.021

Kim KH, Lee W, Kim EE (2016) Crystal structures of human peroxiredoxin 6 in different oxidation states. Biochem Biophys Res Commun 477(4):717–722

Kitano K, Niimura Y, Nishiyama Y, Miki K (1999) Stimulation of peroxidase activity by decamerization related to ionic strength: AhpC protein from Amphibacillus xylanus. J Biochem 126(2):313–319. https://doi.org/10.1093/oxfordjournals.jbchem.a022451

Kristensen P, Rasmussen DE, Kristensen BI (1999) Properties of thiol-specific anti-oxidant protein or calpromotin in solution. Biochem Biophys Res Commun 262(1):127–131. https://doi.org/10.1006/bbrc.1999.1107

Leavitt S, Freire E (2001) Direct measurement of protein binding energetics by isothermal titration calorimetry. Curr Opin Struct Biol 11(5):560–566. https://doi.org/10.1016/s0959-440x(00)00248-7

Liebthal M, Kushwah MS, Kukura P, Dietz KJ (2021) Single molecule mass photometry reveals the dynamic oligomerization of human and plant peroxiredoxins. iScience 24(11):103258. https://doi.org/10.1016/j.isci.2021.103258

Low FM, Hampton MB, Peskin AV, Winterbourn CC (2007) Peroxiredoxin 2 functions as a noncatalytic scavenger of low-level hydrogen peroxide in the erythrocyte. Blood 109(6):2611–2617. https://doi.org/10.1182/blood-2006-09-048728

Manta B, Hugo M, Ortiz C, Ferrer-Sueta G, Trujillo M, Denicola A (2009) The peroxidase and peroxynitrite reductase activity of human erythrocyte peroxiredoxin 2. Arch Biochem Biophys 484(2):146–154. https://doi.org/10.1016/j.abb.2008.11.017

Manta B, Obal G, Ricciardi A, Pritsch O, Denicola A (2011) Tools to evaluate the conformation of protein products. Biotechnol J 6(6):731–741. https://doi.org/10.1002/biot.201100107

Moore RB, Mankad MV, Shriver SK, Mankad VN, Plishker GA (1991) Reconstitution of Ca(2+)-dependent K+ transport in erythrocyte membrane vesicles requires a cytoplasmic protein. J Biol Chem 266(28):18964–18968. https://doi.org/10.1016/S0021-9258(18)55157-7

Nelson KJ, Knutson ST, Soito L, Klomsiri C, Poole LB, Fetrow JS (2011) Analysis of the peroxiredoxin family: using active-site structure and sequence information for global classification and residue analysis. Proteins 79(3):947–964. https://doi.org/10.1002/prot.22936

Orrico F, Möller MN, Cassina A, Denicola A, Thomson L (2018) Kinetic and stoichiometric constraints determine the pathway of H2O2 consumption by red blood cells. Free Radic Biol Med 121:231–239. https://doi.org/10.1016/j.freeradbiomed.2018.05.006

Park JW, Piszczek G, Rhee SG, Chock PB (2011) Glutathionylation of peroxiredoxin I induces decamer to dimers dissociation with concomitant loss of chaperone activity. Biochemistry 50(15):3204–3210. https://doi.org/10.1021/bi101373h

Park MH, Jo M, Kim YR, Lee CK, Hong JT (2016) Roles of peroxiredoxins in cancer, neurodegenerative diseases and inflammatory diseases. Pharmacol Ther 163:1–23. https://doi.org/10.1016/j.pharmthera.2016.03.018

Pastor-Flores D, Talwar D, Pedre B, Dick TP (2020) Real-time monitoring of peroxiredoxin oligomerization dynamics in living cells. Proc Natl Acad Sci U S A 117(28):16313–16323. https://doi.org/10.1073/pnas.1915275117

Peskin AV, Meotti FC, Kean KM, Gobl C, Peixoto AS, Pace PE, Horne CR, Heath SG, Crowther JM, Dobson RCJ, Karplus PA, Winterbourn CC (2021) Modifying the resolving cysteine affects the structure and hydrogen peroxide reactivity of peroxiredoxin 2. J Biol Chem 296:100494. https://doi.org/10.1016/j.jbc.2021.100494

Plishker GA, Chevalier D, Seinsoth L, Moore RB (1992) Calcium-activated potassium transport and high molecular weight forms of calpromotin. J Biol Chem 267(30):21839–21843. https://doi.org/10.1016/S0021-9258(19)36688-8

Randall L, Manta B, Nelson KJ, Santos J, Poole LB, Denicola A (2016) Structural changes upon peroxynitrite-mediated nitration of peroxiredoxin 2; nitrated Prx2 resembles its disulfide-oxidized form. Arch Biochem Biophys 590:101–108. https://doi.org/10.1016/j.abb.2015.11.032

Randall LM, Ferrer-Sueta G, Denicola A (2013) Peroxiredoxins as preferential targets in H2O2-induced signaling. Methods Enzymol 527:41–63. https://doi.org/10.1016/B978-0-12-405882-8.00003-9

Rhee SG, Woo HA (2011) Multiple functions of peroxiredoxins: peroxidases, sensors and regulators of the intracellular messenger H(2)O(2), and protein chaperones. Antioxid Redox Signal 15(3):781–794. https://doi.org/10.1089/ars.2010.3393

Schröder E, Littlechil JA, Lebedev AA, Errington N, Vagin AA, Isupov MN (2000) Crystal structure of decameric 2-Cys peroxiredoxin from human erythrocytes at 1.7 Å resolution. Structure 8(6):605–615. https://doi.org/10.1016/S0969-2126(00)00147-7

Schröder E, Willis AC, Ponting CP (1998) Porcine natural-killer-enhancing factor-B: oligomerisation and identification as a calpain substrate in vitro. Biochim Biophys Acta-Prot Struct Mol Enzymol 1383(2):279–291. https://doi.org/10.1016/S0167-4838(97)00217-3

Schuck P (2013) Analytical ultracentrifugation as a tool for studying protein interactions. Biophys Rev 5(2):159–171. https://doi.org/10.1007/s12551-013-0106-2

Seidel T, Seefeldt B, Sauer M, Dietz KJ (2010) In vivo analysis of the 2-Cys peroxiredoxin oligomeric state by two-step FRET. J Biotechnol 149(4):272–279. https://doi.org/10.1016/j.jbiotec.2010.06.016

Sies H (2017) Hydrogen peroxide as a central redox signaling molecule in physiological oxidative stress: oxidative eustress. Redox Biol 11:613–619. https://doi.org/10.1016/j.redox.2016.12.035

Troussicot L, Burmann BM, Molin M (2021) Structural determinants of multimerization and dissociation in 2-Cys peroxiredoxin chaperone function. Structure 29(7):640–654. https://doi.org/10.1016/j.str.2021.04.007

Veal EA, Underwood ZE, Tomalin LE, Morgan BA, Pillay CS (2018) Hyperoxidation of peroxiredoxins: gain or loss of function? Antioxid Redox Signal 28(7):574–590. https://doi.org/10.1089/ars.2017.7214

Villar, S. F., J. Dalla-Rizza, M. N. Moller, G. Ferrer-Sueta, L. Malacrida, D. M. Jameson and A. Denicola (2022). Fluorescence lifetime phasor analysis of the decamer-dimer equilibrium of human peroxiredoxin 1. Int J Mol Sci 23(9). https://doi.org/10.3390/ijms23095260.

Wang X, Wang L, Wang XE, Sun F, Wang C-C (2012) Structural insights into the peroxidase activity and inactivation of human peroxiredoxin 4. Biochem J 441(1):113–118. https://doi.org/10.1042/BJ20110380

Wood ZA, Poole LB, Hantgan RR, Karplus PA (2002) Dimers to doughnuts: redox-sensitive oligomerization of 2-cysteine peroxiredoxins. Biochemistry 41(17):5493–5504. https://doi.org/10.1021/bi012173m

Wood ZA, Poole LB, Karplus PA (2003a) Peroxiredoxin evolution and the regulation of hydrogen peroxide signaling. Science 300(5619):650–653. https://doi.org/10.1126/science.1080405

Wood ZA, Schroder E, Harris RJ, Poole LB (2003b) Structure, mechanism and regulation of peroxiredoxins. Trends Biochem Sci 28(1):32–40. https://doi.org/10.1016/S0968-0004(02)00003-8

Yewdall NA, Venugopal H, Desfosses A, Abrishami V, Yosaatmadja Y, Hampton MB, Gerrard JA, Goldstone DC, Mitra AK, Radjainia M (2016) Structures of human peroxiredoxin 3 suggest self-chaperoning assembly that maintains catalytic state. Structure 24(7):1120–1129. https://doi.org/10.1016/j.str.2016.04.03

Young G, Hundt N, Cole D, Fineberg A, Andrecka J, Tyler A, Olerinyova A, Ansari A, Marklund EG, Collier MP (2018) Quantitative mass imaging of single biological macromolecules. Science 360(6387):423–427. https://doi.org/10.1126/science.aar5839